Kazemi, Parham; Ponnada, Tushara; Al-Tous, Hanan; Liang, Ying-Chang; Tirkkonen, Olav

# Channel Charting Based Beam SNR Prediction

*Published in:*
2021 Joint European Conference on Networks and Communications & 6G Summit (EuCNC/6G Summit)

*DOI:*
10.1109/EuCNC/6GSummit51104.2021.9482548

Published: 28/07/2021

*Document Version*
Peer reviewed version

*Please cite the original version:*
Kazemi, P., Ponnada, T., Al-Tous, H., Liang, Y-C., & Tirkkonen, O. (2021). Channel Charting Based Beam SNR Prediction. In *2021 Joint European Conference on Networks and Communications & 6G Summit (EuCNC/6G Summit)* (pp. 72-77). [9482548] (European conference on networks and communications). IEEE. https://doi.org/10.1109/EuCNC/6GSummit51104.2021.9482548

# Channel Charting Based Beam SNR Prediction

Parham Kazemi*, Tushara Ponnada*, Hanan Al-Tous*, Ying-Chang Liang†, Olav Tirkkonen*
*Department of Communications and Networking, Aalto University, Espoo, Finland
† University of Electronic Science and Technology of China, Chengdu, P. R. China
Email:{parham.kazemi, tushara.ponnada, hanan.al-tous, olav.tirkkonen}@aalto.fi, liangyc@ieee.org

***Abstract*—We consider machine learning for intra cell beam handovers in mmWave 5GNR systems by leveraging Channel Charting (CC). We develop a base station centric approach for predicting the Signal-to-Noise-Ratio (SNR) of beams. Beam SNRs are predicted based on measured signal at the BS without the need to exchange information with UEs. In an offline training phase, we construct a beam-specific dimensionality reduction of Channel State Information (CSI) to a low-dimensional CC, annotate the CC with beam-wise SNRs and then train SNR predictors for different target beams. In the online phase, we predict target beam SNRs. K-nearest neighbors, Gaussian Process Regression and Neural Network based prediction are considered. Based on SNR difference between the serving and target beams a handover can be decided. To evaluate the efficiency of the proposed framework, we perform simulations for a street segment with synthetically generated CSI. SNR prediction accuracy of average root mean square error less than 0.3 dB is achieved.**

***Index Terms*—beam-management, channel charting, SNR prediction.**

## I. Introduction

Fifth-Generation New Radio (5GNR) is a beam-oriented cellular system, where the network can flexibly configure what beams are used by Base Stations (BSs), and which beams a User Equipment (UE) is aware of. Beamforming is considered the ultimate way to increase the directivity of the antenna to overcome the high path-loss in Millimeter Wave (mmWave) systems and to ensure connectivity [1]. Beam correspondence based on reciprocity between Uplink (UL) and Downlink (DL) is utilized in 5GNR [2]—UL beams can be managed based on information from DL, or vice versa. In Time-Division-Duplex (TDD) systems, this reciprocity can be used for UL/DL beam management if the channel reciprocity meets minimum requirements [3].

User mobility in cellular networks is supported by Handover (HO) procedures. The main phases of 5G HO are the preparation, execution and completion procedures [4]. In mmWave systems, the communication is susceptible to rapid channel fluctuations due to blocking and high shadowing sensitivity. Intra Cell Beam Handovers (ICBH) [5], where beams are switched among a BS's beams, have to be considered in addition to conventional Inter Cell Handovers (ICH). In 5G networks the UE autonomously selects a beam direction both for UL transmission and for DL reception. The UE beam is not under the control of the BS, and without testing with multiple BS–UE beam pairs, the consequences of the change of a BS beam would be unclear. As a result, the BS cannot simply determine the Signal-to-Noise Ratio (SNR) of the best BS beam by measuring the UE transmissions in all the BS beams.

Recently, Machine Learning (ML) algorithms have been applied to beam management. Data driven beamforming in mmWave systems was investigated in [6] where beam directions, beamwidths and transmit powers are found. User mobility is supported by beam tracking. Channel State Information (CSI) history can be used for CSI prediction, which can reduce the overhead of pilots [7]. Moreover, physical location knowledge has been shown to be beneficial in reducing HO signaling overhead [8], and location information of objects surrounding a vehicle can be used for beam power prediction [9].

Channel Charting (CC) [10] is a machine learning framework where dimensionality reduction is applied to collections of massive MIMO CSI, exploiting the massive amounts of CSI available at cellular BSs. In CC, unsupervised ML techniques are used to create a radio map of the cell, which preserves the neighborhood relations of UEs. In [11], we have considered beam-based CC and utilized it for predicting the best beam in a future time-slot. In [12], we have considered HOs based on the predicted SNR; the SNR of a UE from a neighboring BS is predicted based on the relative location information provided by CC. The promising result of SNR prediction in [12] motivates us to consider mmWave beam SNR prediction based on relative locations provided by CC.

In this paper, we focus on ICBH between beams of one BS, and predict beam SNRs based on CC. In an offline phase, beam-specific CCs are created and annotated with SNRs of target beams, and SNR predictors are trained. In the online phase, target beam SNRs are predicted, which can be used to make ICBH decisions. We compare the performance of beam SNR prediction based on CC locations to prediction based on ground truth physical location.

The remainder of this paper is organized as follows. In Section II, the system model and basic CC concepts are introduced. In Section III, network operation for beam SNR prediction using beam CCs is presented. In Section IV, regression techniques for beam SNR prediction are discussed. Numerical results are presented and discussed in Section V. Finally, conclusions are drawn in Section VI.

## II. System Model

We consider a TDD system with a single BS and $U$ UEs in a cell. The BS has an antenna array with $M$ elements, each UE $u$ has an array antenna with $N$ elements. The BS is assumed to have $M$ Radio Frequency (RF) chains for simplicity.

### A. Channel and Beam Model

The MIMO channel between the BS and UE $u$ at a subcarrier is $\mathbf{H}_u \in \mathbb{C}^{M\times N}$. The BS and UEs are capable of beamforming. We assume that the BS codebook has $M$ beams and UE codebook has $N$ beams. Beamforming vectors for the BS are $\mathbf{w}_m \in \mathbb{C}^{M\times 1}$ with $m = 1 \dots M$ and for a UE are $\mathbf{v}_n \in \mathbb{C}^{N\times 1}$ with $n = 1 \dots N$. Wideband beams are assumed at the BS, i.e., the same beam is used for all frequency samples. The UE is capable of using the best beam for every subcarrier. The BS uses a Discrete Fourier Transform (DFT) based codebook of size $M$ and UE uses a DFT codebook of size $N$. The codebook, $\mathbf{C} = [\mathbf{c}_1, \dots, \mathbf{c}_Q]$ is expressed as:

$$\mathbf{c}_q = \frac{1}{\sqrt{Q}}[1, e^{j2\pi\frac{q}{Q}}, \dots, e^{j2\pi\frac{(Q-1)q}{Q}}]^T,\ q = 1, \dots, Q, \quad (1)$$

where $Q = M$ for the BS and $Q = N$ for the UE.

The received signal from UE $u$ when the BS uses beam $m$ and UE uses beam $n$ on the subcarrier is then

$$y^u_{m,n} = \mathbf{w}^H_m \mathbf{H}_u \mathbf{v}_n x + z_u = h^u_{m,n} x + z_u, \quad (2)$$

where $h^u_{m,n}$ represents the effective channel coefficient for BS beam $m$ and UE beam $n$, $x$ is the transmitted symbol with $E\{|x|^2\} = 1$ and $z_u$ is additive white Gaussian noise. The effective channel vector for receiving from UE $u$ using beam $\mathbf{v}_n$, measured from all BS beams is:

$$\mathbf{h}^u_n = \mathbf{W}^H \mathbf{H}_u \mathbf{v}_n, \quad (3)$$

where $\mathbf{W} = [\mathbf{w}_1, \dots, \mathbf{w}_M]$ is the matrix with BS beamforming vectors as columns.

The UE selects it's best beam to transmit towards / receive from a BS beam $\mathbf{w}_m$ using the function:

$$\hat{n} = \hat{n}(m) = \underset{n}{\operatorname{argmax}} |h^u_{m,n}|^2. \quad (4)$$

The effective channel for a transmission from a UE thus depends on which BS beam the UE thinks it is transmitting towards. The average received SNR at BS beam $m$ from a transmissions of UE $u$ towards this beam is then

$$\gamma_{m,u} = \frac{1}{\sigma^2}\,\mathbb{E}\left\{\left|h^u_{m,\hat{n}(m)}\right|^2\right\}, \quad (5)$$

where $\sigma^2$ is the noise power. The expectation is taken over frequency / subcarrier samples and over temporal samples taken from the fast fading process within a short time interval. For a transmission towards BS beam $m$, the effective channel vector from UE $u$, measured from all BS antennas then becomes

$$\mathbf{h}^u_{\hat{n}(m)} = \mathbf{W}^H \mathbf{H}_u \mathbf{v}_{\hat{n}(m)}. \quad (6)$$

If a UE has a single antenna, the best BS beam can be directly measured at the BS. However, when the UE has multiple antennas, and autonomously uses a beamformer, the BS cannot unilaterally measure and find the best beam towards the user. The BS can measure the elements in (6) from UE transmissions, but the BS cannot measure from transmissions towards beam $\mathbf{w}_m$ what the channel coefficients would be if the UE were to transmit towards $\mathbf{w}_{m'}$ with $m' \neq m$. There is a *beam-mismatch problem* arising from UE autonomous precoding; the precoder $\mathbf{v}_{n(m')}$ may or may not be the same as $\mathbf{v}_{n(m)}$.

### B. Basics of Channel Charting

CC [10], [13] is the creation of relative radio maps preserving the neighborhood relations of the UEs in the physical domain. Channel charts are created using channel features that capture the large-scale channel effects. For example, the channel features $\{\boldsymbol{f}_u\}_{u=1}^U$ of the UEs can be extracted from the covariance matrices at the BS.

A dissimilarity Matrix $\mathbf{D}$ is formed at the BS with pairwise CSI dissimilarities between UEs in the cell. Using dimensionality reduction tools and the dissimilarity matrix $\mathbf{D}$, we obtain a representation of the UE locations in the cell which we call a channel chart. We use `ISOMAP` [14] and t-Distributed Stochastic Neighbor Embedding (t-SNE) dimensionality reduction (DR) techniques to obtain the charts. The quality of the obtained CCs is measured by three metrics; Continuity (CT), Trustworthiness (TW) [15] and Kruskal Stress (KS) [16]. CT measures how well the neighbor relations of physical domain are maintained in the representation domain. TW indicates whether false neighbors are avoided in the representation domain. KS indicates how well the global structure is maintained in the representation domain. CT, TW and KS range between 0 and 1, with optimal CT and TW values being 1, and optimal KS being 0.

In order to perform CC in a beam-based system, effective channels measured from multiple beams are needed. This can be done in one shot, if the BS is equipped with multiple RF chains. Here, for simplicity, we assume that the BS is able to measure the effective channel from all of its $M$ beams, obtaining an $M \times 1$-dimensional effective channel $\mathbf{h}^u_{\hat{n}(m)}$ when it measures the output from all $M$ beams with the UE transmitting towards BS beam $m$ using $\hat{n}(m)$. The effective channel will vary depending on which BS beam $\mathbf{w}_m$ the UE is transmitting towards. Due to autonomous UE beamforming the effective channel at the BS is conditioned on the BS beam towards which the UE transmits. To obtain reliable CCs we have to consider a separate CC for each BS beam using the received signals from (6) with UEs transmitting towards the particular BS beam $\mathbf{w}_m$ using UE beam $\mathbf{v}_{\hat{n}(m)}$ that is best for it.

To construct the per-beam CCs, we take a set of sample UEs $\mathcal{K}_m$ transmitting towards beam $\mathbf{w}_m$. We calculate the beam-$m$ specific covariance matrices for these UEs from their effective channels:

$$\mathbf{R}_{m,u} = \mathbb{E}\{\mathbf{h}^u_{\hat{n}(m)}(\mathbf{h}^u_{\hat{n}(m)})^H\}, \quad (7)$$

where $u$ is the UE index. Then beam-specific dissimilarity matrix $\mathbf{D}_m$ is created using the Collinearity Matrix Distance (CMD) metric [17]; the dissimilarity for two UEs $u$ and $u'$ with beam based covariances $\mathbf{R}_{u,m}$ and $\mathbf{R}_{u',m}$ is the Frobenius norm of normalized covariance matrices:

$$d_m(\mathbf{R}_{m,u}, \mathbf{R}_{m,u'}) = 1 - \frac{\mathrm{Tr}(\mathbf{R}_{m,u}\mathbf{R}_{m,u'})}{||\mathbf{R}_{m,u}||_{\mathrm{F}}||\,\mathbf{R}_{m,u'}||_{\mathrm{F}}}, \quad (8)$$

where Tr indicates trace operator. A CC specific for beam $m$ can then be cosnructed from these dissimilarities.

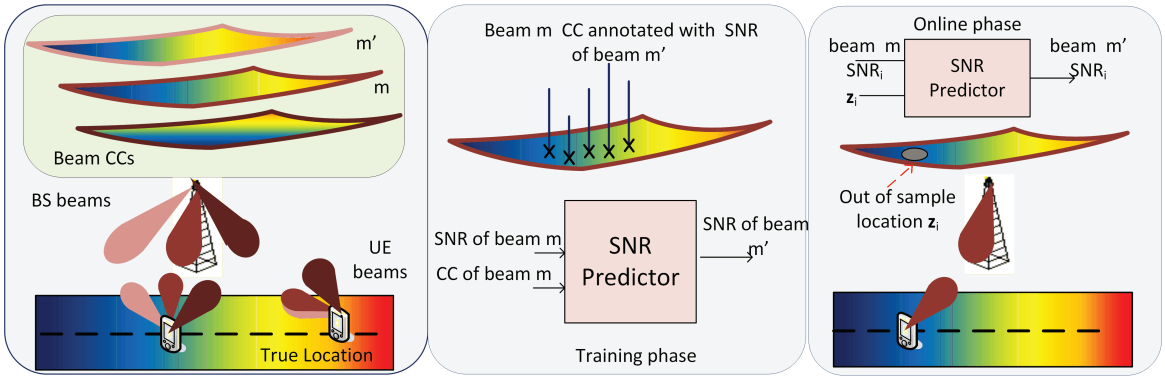


Fig. 1: Beam SNR prediction based on beam CC: (Left); Constructing of beam based CC. (Middle); CC annotation and SNR prediction (the offline phase). (Right); Beam SNR prediction based on beam CC (online phase).

## III. Framework for CC-based Beam-SNR Prediction

In 5GNR, a moving UE may experience switching between several neighboring beams of a given BS. Each beam is considered a cell with its physical and logical channels. Beam handover policies are categorized as either network controlled UE assisted beam switching, in which the BS selects the target beam from measurements performed by the UE, or UE controlled beam switching, in which beam switching is decided by the UE based on measurements [5].

We consider Beam-CC based Network Centric Handover. The basic principle is that each beam has a CC constructed offline and the CC locations are annotated with SNRs of neighboring beams. A prediction algorithm then predicts the SNR of a target beam. The annotated CC and the SNR prediction algorithm are then used to make an ICBH decision. The Network Centric model is illustrated in Figure 1. The Training phase consists of creating channel charts, annotating with neighbor beam SNRs, and training of the SNR predictors. In the online phase, the current beam CC location and SNR are used to predict the SNR at a target beam.

The CC of beam $m$ is denoted as $\mathcal{C}_m$. It is constructed from the covariances $\mathbf{R}_{m,u}$ of the sample UEs $u \in \mathcal{K}_m$ as explained in the previous section. In the annotation step, a subset $\mathcal{K}_{m,m'} = \mathcal{K}_m \bigcap \mathcal{K}_{m'}$ is defined of sample UEs that are present in the CC of both beam $m$ and $m'$. The information of the SNRs $\gamma_{m',u}$ on beam $m'$ is added to the CC-locations in chart $\mathcal{C}_m$ of the users $u \in \mathcal{K}_{m,m'}$. Information across all beam pairs is collected.

Next, using the beam SNRs, the CC locations $\mathcal{C}_m$ for each beam $m$ are divided to groups $\mathcal{T}_{m,m'}$ for $m' \neq m$, as well as $\mathcal{T}_{m,\emptyset}$. If $u \in \mathcal{T}_{m,m'}$, it indicates that for this UE, beam $m'$ is a possible ICBH target beam. If $u \in \mathcal{T}_{m,\emptyset}$, it means that there is no ICBH suggestion for the UE, beam $m$ is definitely the best beam. It should be noted that set $\mathcal{T}_{m,m'}$ may overlap for different $m'$. Each group $\mathcal{T}_{m,m'}$, is assigned to an annotated channel chart $\mathcal{C}_{m,m'}$. For $u \in \mathcal{T}_{m,m'}$, the channel chart location $\mathbf{z}_{m,u} \in \mathcal{C}_{m,m'}$ is annotated with $\gamma_{m',u}$ and $\gamma_{m,u}$.

We have now defined the annotated channel charts $\mathcal{C}_{m,m'}$, where we have CC-locations of users, based on received signals when transmitting towards beam $\mathbf{w}_m$, for which we have SNR information both when transmitting towards $\mathbf{w}_m$ and towards $\mathbf{w}'_m$. Based on this information we learn to predict the SNR of a transmission towards $\mathbf{w}'_m$ given the CSI of transmissions towards target beam $\mathbf{w}_m$. A supervised learning method is used to generate an SNR mapping function $g_{m,m'}(\mathbf{z}_{m,u}, \gamma_{m,u})$ to predict the SNR of the target beam. The SNR mapping for all groups of $\mathcal{T}_{m,m'}$ is developed.

In the online phase, for UE $i$ which has established connection through beam $m$, the obtained SNR mapping function will be used to predict a target beam SNR. First, the beam covariance matrix $\mathbf{R}_{m,i}$ for the UE is estimated at beam $m$. An out-of-sample extension of CC is performed to locate the new UE $i$ on the CC with coordinates $\mathbf{z}_{m,i}$ [18]. Then, the ICBH groups that the UE belongs to are determined based on the CC location $\mathbf{z}_{u,i}$ and the measured SNR $\gamma_{m,i}$. Finally, the SNR for all possible ICBH target beams are predicted. Based on the SNR difference of $\gamma_{m,i}$ and $\gamma_{m',i}$, an ICBH decision is made.

## IV. Algorithms for SNR Prediction

SNR prediction is formulated as a regression problem. Given the annotated beam channel chart $\mathcal{C}_{m,m'}$, the BS finds the function $g_{m,m'}(.)$ to predict the neighboring beam SNR of a UE served by beam $m$. Supervised ML techniques assist us to find this function.

The inputs to the SNR predictor are CC-location $\mathbf{z}_{m,u}$ and the serving beam SNR $\gamma_{m,u}$ for UEs $u \in \mathcal{T}_{m,m'}$. The output is the target beam SNR $\gamma_{m',u}$. We opt for Mean Squared Error (MSE) as the loss function. In this work, K-nearest Neighbors (KNN), Gaussian Process Regression (GPR) and Neural Networks (NN) are considered for prediction.

KNN is a simple non-parametric regression method. The input is the K nearest samples in the training set and the output is the average of the input values. Averaging could be uniform over the K nearest neighbors, or weighted. We consider averaging with uniform weights over $\{1, 3, 10\}$ nearest neighbors.

Gaussian processes are flexible probabilistic models that can be used to perform Bayesian regression without having to provide pre-specified functional relationships between the

TABLE I: Simulation Parameters

| Parameter | Value | Parameter | Value |
|---|---|---|---|
| Center Freq. | 28 GHz | Subcarriers | 256 |
| Subcarrier BW. | 240 KHz | UE speed | 50 Kmph |
| BS Array | 32 ULA | UE Array | 8 ULA |
| Scenario | 3GPP 38.901 UMa-NLOS | BS height | 25 m |

variables [19]. A Gaussian process infers the distribution of the elements of a data set as characterized by its mean and covariance function.

A NN for the problem at hands consists of an input layer, multiple hidden layers, and an output layer, providing one real-valued SNR prediction. The input layer dimension may vary depending on the input feature dimension. We consider three or more real-valued inputs, with 3D input consisting of a 2D channel chart location and the serving beam SNR value. If an $x$D channel chart with $x > 2$ dimensions is used, the input layer will be a $(x+1)$D. Neurons in each layer are fully connected to the next layer and each link has its own weight. The weights are randomly initialized. The learning process has forward and backward propagation. In the feed forward network, the input is propagated across the hidden layers until the output layer. The difference between the predicted output and the given output is minimized using a minimization algorithm. In the back propagation phase, model parameters (weight and bias) will be trained. Stochastic Gradient Descent (SGD) and Levenberg-Marquardt (LM) [20] algorithms are used to minimize the output loss function. The LM algorithm has been shown to be rapidly converging and efficient for moderate sized NNs. However, the computational cost is high as compared to SGD.

The data set is randomly divided into training, validation, and test sets containing 70%, 15%, and 15% of the data samples. The validation set is used for early stopping—as soon as there is no reduction in validation loss we return to the best recorded model parameters. The validation tolerance is set to six iterations. Then, prediction is performed on the test set.

## V. Simulations

The simulation is performed by generating a physical layout and CSI using the Quasi Deterministic Radio Channel Generator (QuaDRiGa) simulator [21]. The layout includes a single BS located at $[-114, -110]$ m, and 2000 UEs scattered randomly in a street segment lying between $[0\ 10]$ m on x-axis and $[0\ 10]$ m on y-axis. The simulation parameters are summarized in Table I.

TABLE II: Average Performance of Beam CCs.

| ISOMAP | | | t-SNE | | |
|---|---|---|---|---|---|
| TW | CT | KS | TW | CT | KS |
| 0.98 | 0.98 | 0.30 | 0.98 | 0.98 | 0.31 |

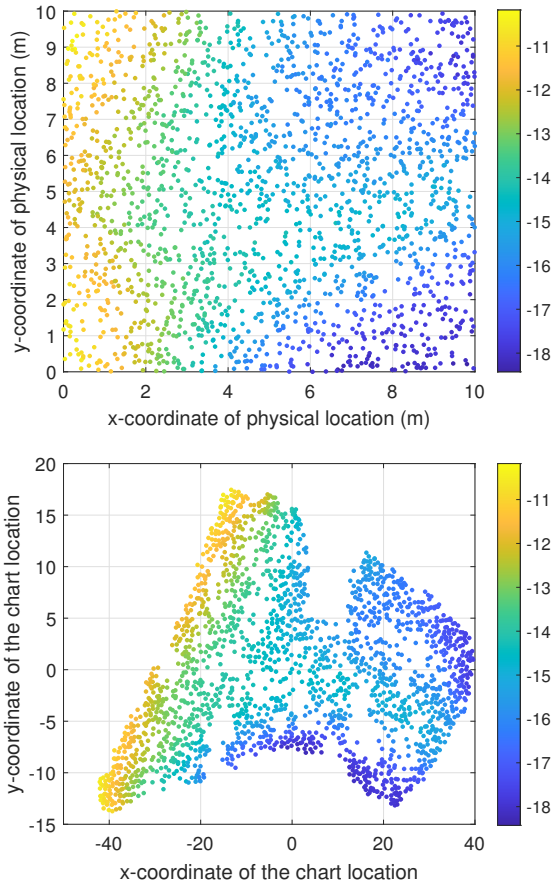


Fig. 2: (Top); Ground truth value of beam 19 SNR at physical locations. (Bottom); t-SNE channel chart of beam 23 annotated with beam 19 SNRs.

### A. Annotated Beam CC

To calculate the covariance matrix, for each UE location we generated 100 small-scale fading temporal samples within a 100 ms timeframe, for UEs moving at 50 km/h. We use CMD to calculate the dissimilarity matrix for each beam, and dimensionality reduction to $x$D using `ISOMAP` and t-SNE.

The CCs obtained are of good quality with the corresponding measures for 2D shown in Table II. CT and TW are computed for 100 neighbors. When increasing dimensions from 2 to 10, CT/TW increase slightly with differences observable in the third digit, while for `ISOMAP`, KS improves from 0.3 to 0.28. CT and TW values are close to 1, which indicates good neighborhood preservation. The CCs also maintain the overall global structure of the UE locations relatively well.

The CCs are then annotated with the beam SNR information measured in the offline phase. An example of a 2D annotated CC is depicted in Fig. 2. The upper part shows the physical location of UEs with their ground truth SNR of beam 19. These SNR values at the t-SNE CC locations of beam 23 are shown in the lower part.

### B. Beam SNR Prediction

SNR mapping functions are created using KNN, GPR and NN predictors. An exponential kernel is considered for the

GPR predictor, and MSE loss function is used. We use NN with three hidden layers, and hyperbolic tangent activation function in the hidden layers. In order to identify an NN structure, we have used the naming scheme, "NNHidden layers-Number of neurons in each hidden layer-Training algorithm", e.g., NN3 10 LM is a NN with three hidden layers and 10 neurons in each hidden layer using LM algorithm to perform back propagation.

The Root Mean Squared Error (RMSE) is used as the performance measure for predictors. The Standard Deviation (std) of the RMSE of different beam pairs' SNR prediction for each predictor is calculated as well. Both are measured from dB-scale SNRs. The input to the predictors has various dimensions, from 2D CC up to 10D CC. In the considered street segment, there are eight dominant beams for which SNR prediction is carried out. The reported average RMSE is averaged over $8\times8$ pairs of beam predictors i.e. for each pair of the beams a predictor is trained.

Figure 3 shows the average RMSE of target beam SNR prediction as a function CC dimension for the test data set, when `ISOMAP` is used for dimensional reduction. The performance of KNN, GPR and NN LM in beam SNR prediction are comparable. For KNN, 10 nearest neighbors has the best performance. The smooth change of SNR in the street segment gives us a good prediction by KNN.

The results show overfitting of NN with LM as the number of neurons in the hidden layer doubles from 10 to 20. Although the training set RMSE is reduced by increasing the hidden layer neurons, the test set RMSE grows. Using SGD, increasing the network size is beneficial. However, the prediction error is almost twice the one of LM. As expected, LM is more effective in optimizing the NN weights. The std of RMSE between different beam pairs for CC based prediction is between 0.06 dB for GPR and 0.07 dB for all NN LM, KNN3 and KNN10, to 0.21 dB for NN 20 SGD. Thus the prediction error of different beam pairs is in an acceptable range and the best predictors—NN3 10/20 LM, KNN10, KNN3 and GPR —are able to perform SNR prediction for all beam pairs equally with almost the same

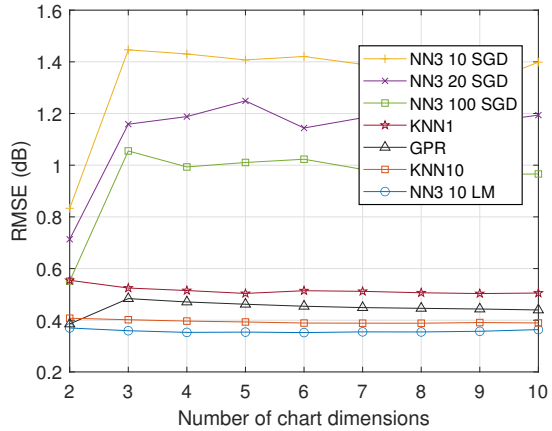


Fig. 3: Average RMSE of different predictors as function of beam CC dimension for `ISOMAP` DR.

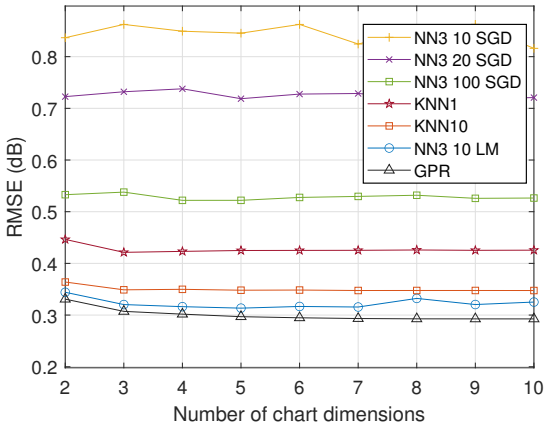


Fig. 4: Average RMSE of different predictors as function of beam CC dimension for t-SNE DR.

precision.

The corresponding performance results for predictors based on t-SNE dimensional reduction can be found in Figure 4. The general trends are the same as in Figure 3 for `ISOMAP`. The t-SNE based predictions have, however, consistently lower RMSE std. GPR is the overall best predictor. For GPR, increasing the dimension of input CC slightly improves the SNR prediction performance.

As a benchmark, we implement prediction based on the true 2D physical location assuming that the physical location is known at the BS [8]. Comparison results can be found in Table III where "Phys Loc." corresponds to the true 2D physical location. For true location based prediction, NN with LM can achieve slightly better performance than KNN and GPR, at the cost of significantly higher computational cost in the training phase. In the simulated scenario, an error floor of 0.25 dB RMSE is found for prediction based on ground truth physical location. GPR using t-SNE CC is the best of the CC-methods, exhibiting a 0.04 dB gap to the ground truth location based prediction.

For controlling ICBH, the dB-domain SNR difference is an important variable. As an example prediction, the SNR of beam 19 is predicted based on the t-SNE CC of beam 23. Figure 5 displays the predicted SNR difference of the two beams vs. the ground truth SNR difference, for a set of sampled UE locations. The prediction is based on NN3 10 LM. The high accuracy of SNR prediction is leading to high accuracy in SNR difference prediction.

TABLE III: Performance of Different Predictors Based on the 2D True Physical Location, 10D `ISOMAP`, and 10D t-SNE CC.

| Predictor | KNN 10 | | GPR | | NN3 10 LM | | NN3 100 SGD | |
|---|---|---|---|---|---|---|---|---|
| | mean | std | mean | std | mean | std | mean | std |
| Phys Loc. | 0.26 | 0.06 | 0.25 | 0.05 | 0.24 | 0.05 | 0.47 | 0.05 |
| t-SNE | 0.35 | 0.06 | 0.29 | 0.05 | 0.32 | 0.06 | 0.52 | 0.06 |
| `ISOMAP` | 0.39 | 0.06 | 0.43 | 0.05 | 0.36 | 0.06 | 1.00 | 0.25 |

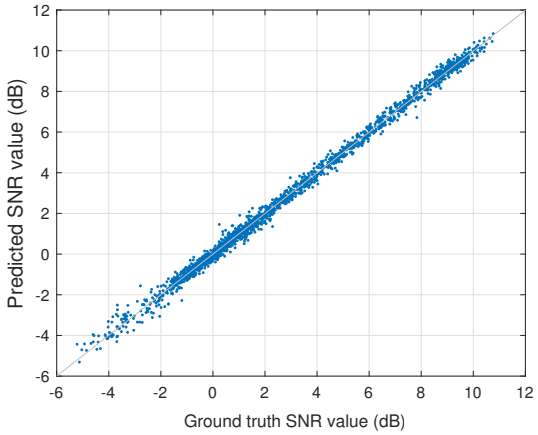

Fig. 5: Prediction value vs ground truth value of beam 19 & 23 SNR difference.

## VI. Conclusion

In this paper, we considered neighboring beam SNR prediction in mmWave systems using a channel chart location derived from dimensionally reduced CSI. Beam-specific channel charts are used, which are radio maps of the received signals of a specific BS beam. A network centric Intra-Cell Beam Handover mechanism is devised where all process are performed at the BS. During a training / offline phase, beam CCs and SNR are gathered and SNR predictors are trained based on annotated CC locations. In the online phase, SNR of the new UE is predicted from received CSI at the BS, and serving beam SNR. K-nearest neighbors, Gaussian process regression and neural networks are used for approximating the SNR mapping function. Levenberg-Marquardt and stochastic gradient descent logarithms are used to train the NN's weights. RMSE has been used as the performance metric. Results show excellent beam SNR prediction accuracy using GPR, and NN with LM. The performance loss of CC based beam SNR prediction, as compared to prediction based on ground truth physical location, is negligible. For NN based prediction, increasing the number of hidden layers and / or neurons is not beneficial for the considered data set. Overall, the best prediction performance was found with GPR using t-SNE CC, which predicts within a 0.05 dB gap of the best predictor based on ground truth physical location. When it comes to CC-dimensionality, there is little gain from using a CC with more than 3 dimensions. In future work, the intra-cell beam SNR prediction approach discussed here will be extended to inter-cell beam SNR prediction.

## Acknowledgment

This work was funded in part by the European Union under the framework of the project H2020-MSCA-ITN 813999 Windmill and the Academy of Finland (grant 319484).

## References

[1] M. Giordani, M. Polese, A. Roy, D. Castor, and M. Zorzi, "A tutorial on beam management for 3GPP NR at mmWave frequencies," *IEEE Commun. Surveys Tuts.*, vol. 21, no. 1, pp. 173–196, 2019.

[2] 3GPP, "Study on new radio (NR) access technology," 3rd Generation Partnership Project (3GPP), Technical document number 38.912, version 14.0.0, May 2017.

[3] Y. R. Li, B. Gao, X. Zhang, and K. Huang, "Beam management in millimeter-wave communications for 5G and beyond," *IEEE Access*, vol. 8, pp. 13 282–13 293, 2020.

[4] M. Tayyab, X. Gelabert, and R. Jantti, "A survey on handover management: From LTE to NR," *IEEE Access*, vol. 7, pp. 118 907–118 930, 2019.

[5] N. W. Sung and Y. S. Choi, "Fast intra-beam switching scheme using common contention channels in millimeter-wave based cellular systems," in *Proc. Internat. Conf. Advanced Commun. Technol (ICACT)*, Jan. 2016, pp. 760–765.

[6] P. Zhou, X. Fang, X. Wang, Y. Long, R. He, and X. Han, "Deep learning-based beam management and interference coordination in dense mmwave networks," *IEEE Trans. Veh. Technol.*, vol. 68, no. 1, pp. 592–603, 2019.

[7] Y. Guo, Z. Wang, M. Li, and Q. Liu, "Machine learning based mmwave channel tracking in vehicular scenario," in *Proc. of IEEE ICC Workshops*, 2019, pp. 1–6.

[8] M. Arvinte, M. Tavares, and D. Samardzija, "Beam management in 5G NR using geolocation side information," in *Proc. of Conf. Information Sciences and Systems (CISS)*, 2019, pp. 1–6.

[9] Y. Wang, M. Narasimha, and R. W. Heath, "Mmwave beam prediction with situational awareness: A machine learning approach," in *Proc. of IEEE (SPAWC)*, 2018, pp. 1–5.

[10] C. Studer, S. Medjkouh, E. Gönültaş, T. Goldstein, and O. Tirkkonen, "Channel charting: Locating users within the radio environment using channel state information," *IEEE Access*, vol. 6, pp. 47 682–47 698, 2018.

[11] T. Ponnada, H. Al-Tous, and O. Tirkkonen, "Location-free beam prediction in mmWave systems," in *IEEE VTC-Spring*, 2021, pp. 1–6.

[12] P. Kazemi, H. Al-Tous, C. Studer, and O. Tirkkonen, "SNR prediction in cellular systems based on channel charting," in *Proc. of the IEEE Internat. Conf. on Commun. and Networking (ComNet)*, 2020, pp. 1–8.

[13] J. Deng, S. Medjkouh, N. Malm, O. Tirkkonen, and C. Studer, "Multipoint channel charting for wireless networks," in *Proc. of Asilomar Conf. on Signals, Systems, and Computers*, Oct. 2018, pp. 286–290.

[14] J. B. Tenenbaum, V. De Silva, and J. C. Langford, "A global geometric framework for nonlinear dimensionality reduction," *Science*, vol. 290, no. 5500, pp. 2319–2323, 2000.

[15] J. Venna and S. Kaski, "Neighborhood preservation in nonlinear projection methods: An experimental study," in *Proc. of the International Conference on Artificial Neural Networks, (ICANN)*, 2001, pp. 485–491.

[16] J. B. Kruskal, "Multidimensional scaling by optimizing goodness of fit to a nonmetric hypothesis," *Psychometrika*, vol. 29, pp. 1–27, 1964.

[17] M. Kurras, S. Dai, S. Jaeckel, and L. Thiele, "Evaluation of the spatial consistency feature in the 3GPP geometry-based stochastic channel model," in *Proc. of IEEE WCNC*, Apr. 2019, pp. 1–6.

[18] T. Ponnada, H. Al-Tous, O. Tirkkonen, and C. Studer, "An out-of-sample extension for wireless multipoint channel charting," in *Proc. of EAI Internat. Conf. on Cognitive Radio Oriented Wireless Networks,(Crowncom)*, Jun. 2019.

[19] C. K. Williams and C. E. Rasmussen, *Gaussian processes for machine learning*. Cambridge, MA: MIT press, 2006.

[20] M. T. Hagan and M. B. Menhaj, "Training feedforward networks with the marquardt algorithm," *IEEE Trans. Neural Networks*, vol. 5, no. 6, pp. 989–993, 1994.

[21] S. Jaeckel, L. Raschkowski, K. Borner, and L. Thiele, "QuaDRiGa: A 3-D multi-cell channel model with time evolution for enabling virtual field trials," *IEEE Trans. Antennas Propag.*, vol. 62, no. 6, pp. 3242–3256, Jun. 2014.